Alkali-Activated Foams Coated with Colloidal Ag for Point-of-Use Water Disinfection

Bhuyan, Mohammad Amzad Hossain; Karkman, Antti; Prokkola, Hanna; Chen, Boyu; Perumal, Priyadharshini; Luukkonen, Tero

DOI
10.1021/acsestwater.3c00711

Publication date
2024

Document Version
Final published version

Published in
ACS ES and T Water

ACS ES&T Water

pubs.acs.org/estwater

Article

Alkali-Activated Foams Coated with Colloidal Ag for Point-of-Use Water Disinfection

Mohammad Amzad Hossain Bhuyan, Antti Karkman, Hanna Prokkola, Boyu Chen, Priyadharshini Perumal, and Tero Luukkonen*

Cite This: *ACS EST Water* 2024, 4, 687−697

Read Online

ACCESS | Metrics & More | Article Recommendations | Supporting Information

ABSTRACT: Alkali-activated foams are ceramic-like materials prepared at near-ambient temperature. This study investigates them for point-of-use water disinfection, thus providing an alternative to ceramic filters fired at a high temperature. Alkali-activated foams with different compositions were characterized for the porosity, mechanical strength, shrinkage, and microstructure. The optimized foam, employing metakaolin as the raw material, was coated with a colloidal Ag solution. The disinfection performance and leaching behavior of the foams was followed in a continuous 10 week experiment, where clean water with a weekly pulse of contaminated water was distributed through the foam. The average inactivation of *Escherichia coli* with the Ag-coated foam was 2.84 $\log_{10}$, which was 1.27 units higher compared to foam without Ag. A quantitative polymerase chain reaction analysis and metagenomic sequencing verified that foams with and without Ag were both capable of reducing the microbial load. Furthermore, the changes induced by the foam with Ag on the microbial community composition, antibiotic resistome, and metal and biocide resistomes were significant. The leached concentrations of Ag, Na, Si, and Al were in accordance with the drinking water guidelines. Finally, a life cycle assessment indicated the possibility of reducing the global warming potential and the total embodied energy in comparison with a conventional ceramic filter.

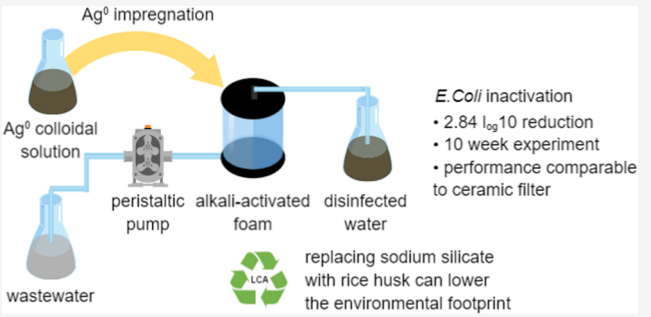

KEYWORDS: *alkali-activated materials, geopolymers, point-of-use water treatment, water disinfection, water supply*

1. INTRODUCTION

Safe drinking water is a key part of the United Nations sustainable development goal no. 6 (*Ensure availability and sustainable management of water and sanitation for all*). Specifically, the presence of pathogenic microbes in drinking water is of great concern regarding health.[1] Globally, almost 200 million people do not have adequate access to safe drinking water.[1] In this context, point-of-use (POU) drinking water treatment using Ag-coated ceramic filters in households has become an important practice in developing countries.[2] Ceramic filters can remove or inactivate bacteria, protozoa, and, to a limited extent, viruses.[2−6] These filters are manufactured using locally available raw materials (i.e., clay and organic combustible materials) with added Ag and are cost-effective in comparison with a centralized water treatment.[7,8] However, there are some issues associated with ceramic filters, including difficulties in maintaining a high flow rate over an extended service period, insufficient removal of diverse water pollutants (e.g., toxic metals), and the need for firing (at up to ∼1000 °C for several hours). The firing may cause smog and particulate matter emissions, especially when using low-quality fuels in firing kilns.[7−9] To address these issues, ceramic POU filters have been further developed recently by replacing Ag with La(III) to improve bacteria and virus inactivation.[10−12] On the other hand, the flow rate in such filters can be improved by carefully selecting a combustible organic material, such as recycled paper fiber, which has shown promising performance.[13]

Alkali-activated materials (AAMs), including their subgroup "geopolymers," could provide an alternative to conventional ceramic filters with potential benefits arising from their low-temperature manufacturing process. AAMs are amorphous aluminosilicates consisting of cross-linked chains or 3D networks of tetrahedral AlO_4 and SiO_4 and charge-balancing cations such as Na^+.[14,15] A wide range of materials, such as fly and bottom ashes, calcined clay minerals, or metallurgical slags with soluble Si and Al at alkaline conditions, can be used as precursors in the preparation of AAMs.[16] Depending on their composition and preparation method, AAMs can exhibit low

Received: November 13, 2023
Revised: January 9, 2024
Accepted: January 9, 2024
Published: January 20, 2024

environmental footprint, cation exchange capacity, high water permeability, and mesoporous structure.[17−20] Highly porous alkali-activated foams (AAFs) can be fabricated using the direct foaming method, where a blowing agent (such as H_2O_2) and a surfactant are added to fresh-state paste, resulting in pore structure formation. Although the application of AAFs to wastewater treatment as adsorbents has been widely studied,[21−25] their application to water disinfection has received less attention. Antimicrobial properties can be introduced to AAMs, for example, by the ion exchange of charge-balancing cations (e.g., Na^+) with Ag^+.[26] Also, it was recently reported that a composite AAM structure with bentonite containing Ag nanoparticles can be successfully used in water disinfection. However, its disinfection efficiency decreases quickly.[14]

In this study, AAFs were prepared using the direct foaming method and functionalized by applying a colloidal silver solution on their surface. The most promising foam sample was studied as a POU water disinfection filter. The objectives of this study are to (i) prepare and optimize AAFs representing typical high-, low-, and medium-Ca gel compositions using blast furnace slag, metakaolin, or a mixture of these two, respectively, and compare their properties (i.e., mechanical strength, porosity, and microstructure), (ii) characterize the performance of the optimized foam sample after modifying the colloidal Ag in *Escherichia coli* (*E. coli*) inactivation, and (iii) investigate how the bacterial abundance and microbiome composition are altered by AAFs with and without Ag using a quantitative polymerase chain reaction (qPCR) analysis and metagenomic sequencing, and (iv) evaluate the environmental sustainability of AAFs in comparison to that achieved by ceramic filters by conducting a life cycle assessment (LCA).

2. METHODS AND MATERIALS

2.1. Materials and Chemicals. Metakaolin (MK) and blast furnace slag (BFS) were used as the aluminosilicate precursors. Details of the composition of MK and BFS are provided in the Supporting Information. A mixture of sodium silicate solution (7.5−8.5 weight-% Na_2O and 25.5−28.5% SiO_2, Merck) and sodium hydroxide pellets (98.7%, VWR) was used as an alkali-activator solution with a molar ratio of $SiO_2/Na_2O \approx 1.2$. H_2O_2 (30%, VWR, w/v) and sodium dodecyl sulfate (SDS) (10% aqueous solution, Merck) were used as a blowing agent and a surfactant, respectively, in the foam preparation using the direct foaming method. Acetic acid was used to neutralize the residual alkalinity in the pore solution of the foam. The foam was coated with colloidal Ag solution obtained from Argenol Laboratories (Spain).

2.2. Preparation of Foam Samples and Ag Application. Three types of AAFs, using BFS, MK, or a mixture of BFS and MK as precursors, were prepared by applying the direct foaming method.[27] The weight ratios of the raw materials are shown in Table S1 in Supporting Information. To achieve a constant headwater permeability coefficient comparable to that of conventional ceramic filters (i.e., ∼0.0037 cm/s),[28] the amount of H_2O_2 solution was varied, as shown in Table S1. Based on the amount of H_2O_2 used, AAFs are labeled as BFS-1, BFS-2, BFS-3, MK-1, MK-2, MK-3, MK-4, BFS-MK-1, BFS-MK-2, BFS-MK-3, and BFS-MK-4. The foam samples were characterized by compressive strength, flexural strength, and shrinkage, and details of processes are discussed in Supporting Information.

The pore solution of the optimized AAF sample (i.e., MK-1 in Table S1) was neutralized by distributing 2 L of 0.1 M acetic acid with a flow rate of 1 L/h through the sample, followed by deionized water flushing. Thirty mL of a colloidal Ag solution (800 ppm) was applied to the optimized AAF sample using a peristaltic pump to fill the pore space.[29] Then, the sample was left to stand at room temperature for approximately 17 h. Next, the sample was flushed using 0.5 L of deionized water and used in the disinfection experiment. A diagram of the preparation of the foam samples and Ag application is shown in Figure S1 (Supporting Information).

2.3. Disinfection Experiment. A disinfection experiment was conducted to evaluate the mechanical durability, leaching of ions, and disinfection performance of the foam samples over a 10 week period. On a daily basis, 5 L of deionized water were distributed through the foam samples (⌀ = 4.3 cm, height = 10.2 cm) with or without Ag using a peristaltic pump (flow rate: 1 L/h). Thus, the empty bed contact time was ∼9 min. A diagram about the experimental setup is shown in Figure S2 (Supporting Information). A daily sample of deionized water obtained after filtration was collected and analyzed for Ag, Si, Al, and Na using XSeries II ICP−MS (Thermo Fisher Scientific), according to the ISO 17294-2:2016 (ISO, 2016) standard.[30] Also, its pH was measured using a Hach HQ11d/PHC10101. Each day, after 5 L of deionized water was pumped, the pump was stopped and the water was allowed to stand in the foam until the next day. Once per week, a 1 L pulse of tertiary-treated nondisinfected municipal wastewater (collected weekly from the Taskila wastewater treatment plant, Oulu, Finland, for which the process has been described in ref 14) was distributed through the foam samples. A duplicate sample of wastewater was collected before and after filtration in sterilized plastic containers and analyzed for *E. coli*, according to the ISO 9308-1 (ISO, 2014) standard.[31] The samples were preserved at ≤4 °C, and the analysis was initiated within 24 h of sampling. Foam samples were further analyzed before and after the disinfection experiment by using a field emission scanning electron microscope (FESEM) and X-ray photoelectron spectroscopy (XPS). XPS spectra can be found in the Supporting Information. The wastewater samples used in the experiment were assessed for absorbance at 256 nm, total solids, total organic carbon (TOC), seven-day biological oxygen demand (BOD_7), and turbidity within 2 h of sampling (Table S2). Details are provided in the Supporting Information.

2.4. DNA Extraction, qPCR, and Metagenomic Sequencing. 200 mL of wastewater were collected before and after POU filtration and filtered through a 0.2 μm tract-etched membrane (Whatman). The filter papers were preserved in a freezer at −10 °C until DNA extraction. DNA was extracted from the filtration membranes using a DNeasy PowerWater kit (Qiagen) according to the manufacturer protocol. Bacterial 16S rRNA gene copy numbers were quantified using qPCR and primers pA and 358R.[32,33] A standard curve for qPCR was constructed using a 10-fold dilution series of linearized pUC57 plasmid DNA containing a 1542-bp fragment of *E. coli* 16S rRNA gene.[34] All qPCR reactions were run in triplicate on a 96-well plate using a QuantStudio 3 System (Thermo Fisher Scientific). The mean and standard deviation of the technical replicates were used in all of the further analyses. Metagenomic sequencing was conducted for all samples. For a detailed description of the

https://doi.org/10.1021/acsestwater.3c00711
ACS EST Water 2024, 4, 687−697

qPCR and metagenomic sequencing, see text in Supporting Information.

2.5. Bioinformatic Analysis. Sequencing adapters were trimmed using Cutadapt v.3.5.[35] The microbial community composition was analyzed using MetaPhlAn v.4.0.3.[36] Antibiotic resistance genes (ARGs) were annotated by mapping reads against the ResFinder database v.2.0.0[37] using Bowtie v.2.4.4[38] and Samtools v.1.16.1.[39] Metal and biocide resistance genes (MBRGs) were annotated using Diamond v. 2.0.15[40] and the BacMet2 database.[41]

2.6. Statistical Analysis. All statistical analyses were conducted using R v. 4.2.2.[42] The 16S rRNA gene quantification with qPCR was used as a proxy for bacterial abundance in the samples and for calculating the absolute abundance of features. The difference between bacterial counts between wastewater and the two filtrates was tested by employing a linear mixed-effect model using function *lmer* from lme4 v.1.1-31.[43] The counts were log-transformed. The sampling week was used as a random effect, and the sample type was used as a fixed effect. For a pairwise comparison, Tukey's posthoc test was performed using function *glht* from multcomp v.1.4-22.[44] The changes in the community compositions were tested by performing a permutational multivariate analysis of variance using Euclidean distances with function *adonis2* from vegan v.2.6-4.[45] The *p*-values were corrected for multiple testing via the BH method using *p.adjust* in stats.[42] Ordinations were constructed with function *cmdscale* from stats[42] using Euclidean distances calculated with *vegdist*.[45] The differential abundance of features was tested in a pairwise manner by employing linear mixed-effect models using function *Maaslin2* from Maaslin2 v. 1.12.0.[46] The results were visualized using the ggplot2 v. 3.4.0,[47] patchwork v.1.1.2,[48] and microViz v.0.10.4[49] packages. Only results with a *p*-value <0.05 were reported as significant. For a detailed description of the statistical methods used, see text (Supporting Information).

2.7. Life Cycle Assessment (LCA). LCA was conducted to compare the environmental impact of alkali-activated POU foam samples and that of a conventional ceramic POU water filter reported earlier.[9] LCA focused on the global warming potential (GWP) and the embodied energy (EE) due to the lack of data provided by other indicators for rice husk ash. LCA was performed according to the ISO 14040[50] and EN 15804[51] standards. The functional unit selected was 1000 g of the POU foam/filter material. The cradle-to-gate LCA, which only deals with the raw material supply and manufacturing process in the production stage, was performed according to three scenarios (Table 1). The manufacturing process considers the thermal curing of a MK foam sample and firing of a ceramic water filter. Scenario 1 (GP1) represents the optimum mixture used in this study (the physical form or composition of some raw materials was slightly changed to match them with the database materials). Scenario 2 (GP2) is similar, but the sodium silicate solution was replaced with rice husk ash and sodium hydroxide. Scenario 3 (CER) represents the typical ceramic filter raw materials and the firing process reported earlier.[7,9] For a detailed description of LCA, see the text and Table S3 in Supporting Information.

3. RESULTS AND DISCUSSION

3.1. Comparison of Aluminosilicate Precursors and Optimization of the Foam Sample Porosity. To compare the different AAF samples, their constant head water permeability coefficient was adjusted to a value similar to that representing the upper bound of values reported for conventional POU ceramic filters, that is, ∼0.0037 cm/s [Figure 1a].[28] In Figure 1a, the light blue region indicates the typical constant head water permeability coefficient range for the conventional POU ceramic filters. The water permeability depends on the porosity and pore structure of the material. In AAFs, the amount of a blowing agent can be controlled (i.e., H_2O_2 in this case). H_2O_2 decomposes into O_2 gas bubbles at high-pH conditions of a fresh-state alkali-activated paste.[18] In addition, a surfactant prevents the escape and coalescence of gas bubbles from the fresh-state alkali-activated paste by reducing the surface tension of the air−paste interface (i.e., reducing the Laplace pressure) and stabilizing them inside the paste.[52,53] At the same time, the gas bubbles are joined together into interconnected voids by the action of the surfactant (i.e., SDS in this study) and eventually form the pore structure upon hardening.[18] By decreasing the amount of H_2O_2, the porosity and pore sizes of the foam samples decrease, thus, reducing the water permeability. Figure 1a shows that the dose of H_2O_2 required to achieve the desired water permeability varies depending on the foam composition. This is probably due to the differences in alkalinity, rheology, and setting behavior of the foam samples.[54]

Table 1. Materials and Curing/Firing Process Used for the Preparation of Alkali-Activated Foam Samples and Ceramic POU Water Filters

material [wt ratio]	metakaolin-based water filter		ceramic water filter
	scenario 1 (GP1)	scenario 2 (GP2)	scenario 3 (CER)
metakaolin	1	1	
kaolinite clay			1
rice husk ash		0.33	
saw dust			0.32
laterite soil			0.03
sodium silicate (solution, SiO_2/Na_2O = 3.5)	1.19		
NaOH pellets	0.18	0.30	
silver (as 100% metal)	4.74×10^{-5}	4.81×10^{-5}	3.7×10^{-5}
50% H_2O_2	6.19×10^{-3}	6.18×10^{-3}	
surfactant (10% solution)	1.99×10^{-3}	2.02×10^{-3}	
water		0.77	0.49
curing or firing temperature and duration	60°C, 4 h	60°C, 4 h	800°C, 10 h

The porosity of the POU filter materials also contributes to the physical separation of pathogens. It has been estimated that conventional ceramic filters can separate up to 99.97% of *E. coli* without employing Ag.[29,55,56] Furthermore, it has been suggested that ceramic filters without Ag can develop biofilms and filter cake on their surface, thus enhancing the microbe separation.[57] Based on the optimization of the H_2O_2 amount, foam samples BFS-1, MK-1, and BFS-MK-1 were selected for further investigation. From now on, foam samples BFS-1, MK-1, and BFS-MK-1 will be referred to as BFS, MK, and BFS−MK, respectively.

3.2. Shrinkage. Shrinkage in AAF samples when used as filters for POU water treatment is important, because it can lead to cracking. Shrinkage can be mitigated by decreasing the filter dimensions or by using fiber reinforcements. Drying shrinkage is the result of evaporation of weakly bound water molecules, whereas autogenous shrinkage is the result of water

https://doi.org/10.1021/acsestwater.3c00711
ACS EST Water 2024, 4, 687−697

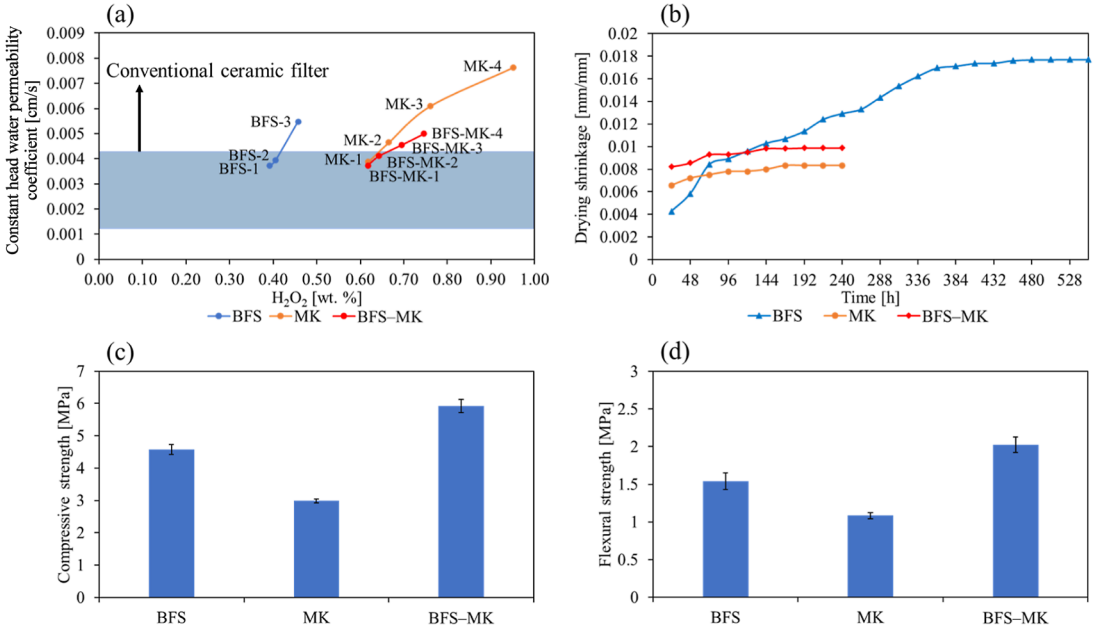

Figure 1. (a) Effect of the amount of H_2O_2 on the constant headwater permeability coefficient in AAFs. The targeted value of the coefficient is shown with the blue area in the figure: (b) comparison of length change in three different AAFs (BFS, MK, and BFS−MK) with time, (c) comparison of compressive strength (MPa), and (d) comparison of flexural strength (MPa).

consumption during the formation of new mineral phases such as alkali or alkaline earth metal aluminosilicate gels.[58] Therefore, shrinkage (i.e., length change) in AAFs using the optimum H_2O_2 amount was studied at ambient conditions up to the point it reached a constant value [Figure 1b]. For example, the porosity, composition, and curing conditions of the material affect the length change.[59] The BFS-based foam sample clearly exhibited the highest shrinkage compared to the other two foam samples. Earlier studies that compared MK and BFS-based AAMs have shown that in the BFS foam, water can be lost through mesopores, causing internal capillary stress.[60] This stress is higher in BFS-based AAM samples than that in MK-based AAM samples and can contribute to a higher length reduction (or shrinkage) in a BFS foam sample than in an MK foam sample.[60] The measured shrinkage in high- and medium-Ca foams, BFS, and BFS−MK foams was higher than that in low-Ca foams. These results are similar to those reported in an earlier study.[58] Based on the shrinkage results, the MK foam was selected for disinfection and further study.

3.3. Mechanical Strength. A compressive strength in the 0.9−1.7 MPa range and a flexural strength in the 1.0−4.7 MPa range are considered sufficient for materials intended for POU water treatment since these values ensure integrity in operating conditions.[61−65] These values can be obtained for all mixtures of foam samples [Figure 1c,d]. The mechanical strength of the porous body is dependent on the pore structure. i.e., large pores or high porosity decrease the mechanical strength.[66] The highest average compressive strength was observed in the MK−BFS mixture (i.e., the medium-Ca mixture). The lower porosity of BFS−MK mixture (≈58%) compared to BFS foam (≈70%) and MK foam (≈77%) could explain this. The differences in the gel structure, that is, the coexistence of zeolite-like phases in the low-Ca mixture and tobermorite-like phases in the medium-Ca mixture, were mainly responsible for the higher compressive strength and flexural strength values of the BFS−MK mixture compared with those of the MK and BFS foam samples.[67] Also, the average compressive strength of the BFS foam sample was higher than that of the MK foam sample. This difference can be explained by the more compact microstructure of the BFS foam compared with that of the MK foam and the presence of Ca in the BFS foam.[60] Additionally, the low compressive strength of the MK foam sample can be attributed to its high water demand and water evaporation.[60] The flexural strength follows a trend similar to that of the compressive strength.

3.4. Disinfection Performance. *3.4.1. Enumeration of Viable E. coli.* To inactivate *E. coli*, the MK foam was modified using Ag. From an XRF analysis, the Ag loading was determined to be approximately 0.024 wt % (0.24 mg/g). Modified and nonmodified foam samples have been referred to as MK−Ag and MK foam samples, respectively. The inactivation of *E. coli* using the MK−Ag foam sample remained high ($\log_{10}$ reduction > 2.5) until the fifth week. During this time, ∼180 L of water was treated (i.e., 1208 empty bed volumes), of which 5 L was contaminated water and 175 L was clean water to demonstrate the leaching stability of the filter. It should be noted though that during the first 3 weeks, the accurate quantification of logarithmic *E. coli* inactivation could not be achieved since the *E. coli* enumeration results were <100 CFU/100 mL (CFU: colony-forming unit) due to reasons related to the sample dilution. Nevertheless, the qPCR results confirmed that the bacterial load and inactivation results during the first 3 weeks were comparable to those in week 4 [Figure 2a]. Another important observation was the significant variation in the wastewater *E. coli* amount (range: 800−170,000 CFU/100 mL). The *E. coli* amount of the present study is comparable to some contaminated river water reported in the literature.[68] By increasing the influent *E. coli* amount, the $\log_{10}$ inactivation value also increased, indicating that the foam was capable of coping with variable loads. The MK foam followed a trend similar to that of MK−Ag, except that the $\log_{10}$ reduction was ∼50% lower until week 7. From then on, the *E. coli* inactivation using both foam samples was approximately the same, indicating that the Ag coating was

https://doi.org/10.1021/acsestwater.3c00711
ACS EST Water 2024, 4, 687−697

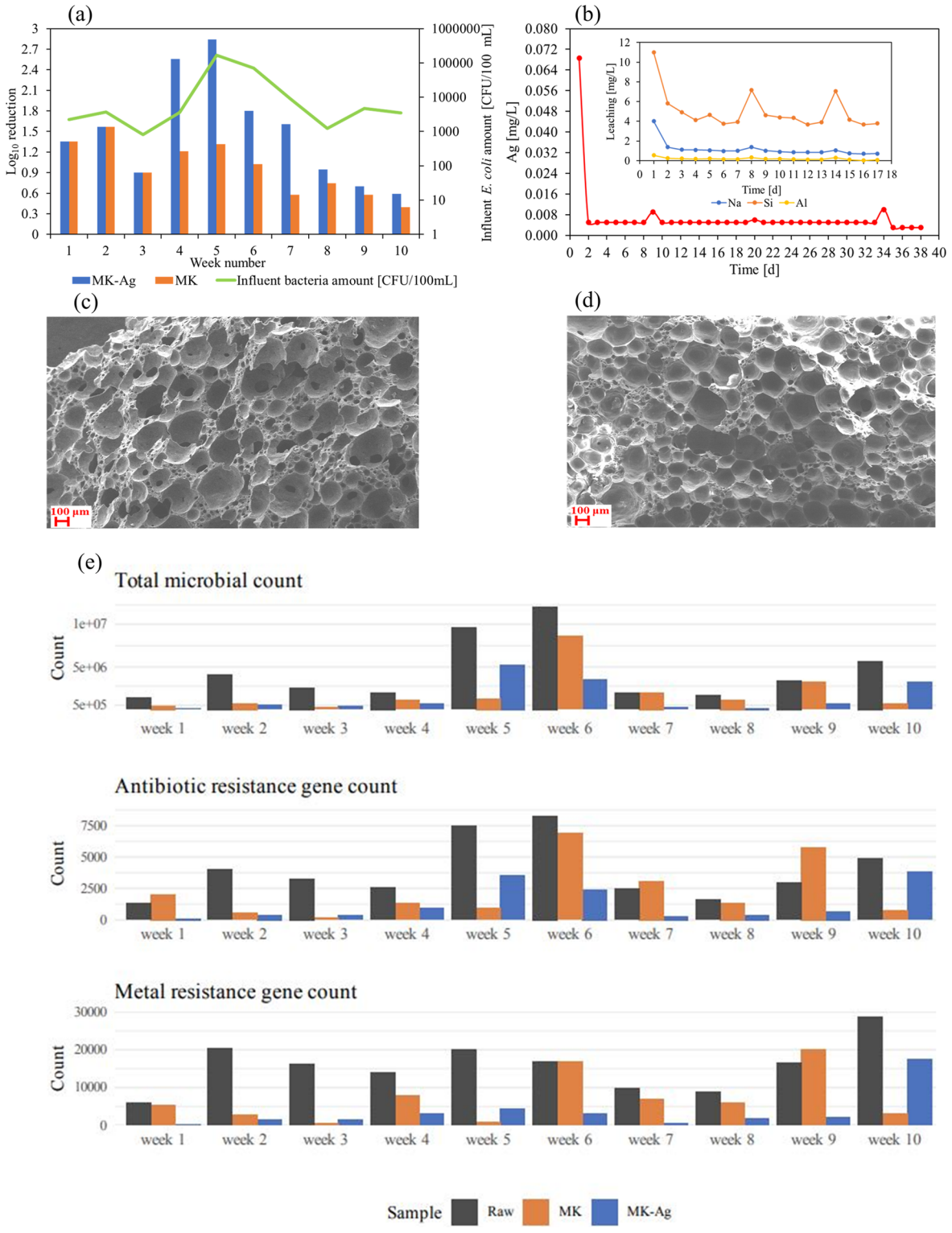

Figure 2. (a) *E. coli* bacteria inactivation in wastewater during a 10 week disinfection experiment using MK-based geopolymer foam with and without colloidal Ag on its surface. (*The log reduction values in the first 3 weeks were not accurately known, i.e., the *E. coli* enumeration results were <100 CFU/100 mL due to reasons related to sample dilution; thus, the indicated values refer to a minimum $\log_{10}$ reduction.) (b) Leaching of Ag, Na, Si, and Al obtained from the alkali-activated MK foam over a 10-week experiment. (c, d) SEM micrograph of MK-Ag foam before and after disinfection experiment. (e) Total microbial counts, antibiotic resistance gene (ARG) counts, and metal and biocide resistance gene (MBRG) counts in input wastewater (raw) and in MK foam-based filters with (MK−Ag) and without (MK) Ag. Counts are based on 16S rRNA gene qPCR results.

leached out of the material (see Section 3.5), which also happens in conventional ceramic filters. The XPS analysis of the foam material before and after the disinfection experiment confirmed that ~90% of Ag was leached out of the filter. The XPS spectrum of Ag in the MK−Ag foam sample before and after the disinfection experiment is shown in Figure S3

https://doi.org/10.1021/acsestwater.3c00711
ACS EST Water 2024, 4, 687−697

(Supporting Information). In the end of the 10 week experiment, the $\log_{10}$ reduction values for the MK-based foam sample with and without Ag were 0.59 and 0.40, respectively. The disinfection efficiency could be likely revived by reapplying the Ag colloidal solution to the foam surface similarly as with conventional ceramic filters.[69] The pH of the wastewater pulses before and after filtration remained stable in the 6−7 range throughout the 10 week experiment.

The *E. coli* inactivation using nonmodified foam probably represents the capability of foam to physically separate bacteria. The highest *E. coli* inactivation using the Ag-coated foam was 2.84 $\log_{10}$ (~99.9% removal), and that using the MK foam without modification was 1.57 $\log_{10}$ (~96% removal).

The bacterial inactivation using the Ag-coated foam was higher than that reported in ref 14, where the log reduction using the Ag-modified foam was up to 2.4 $\log_{10}$, and it decreased after 7 h when in contact with the wastewater used in our study. The improved performance achieved in our study indicates that the changes in the pore structure (smaller pores) were caused by an amount of blowing agent (H_2O_2) lower than that used in previous study.[14] Also, by applying the Ag colloidal solution to the surface of the foam instead of applying bentonite−Ag nanoparticles to the fresh-state paste during preparation contributed to an improved and long-lasting inactivation.

The results obtained in our study are comparable to the $\log_{10}$ reduction results of *E. coli* (typical range: 2−5 $\log_{10}$[8,29,69]) obtained from a POU ceramic filter prepared at high temperature and modified with colloidal Ag. In that case, Ag was applied to the filter by brushing or the filter was submerged into the colloidal Ag solution, which is essentially a method similar to that applied here. The SEM micrographs showed no visible differences, indicating that after 10 weeks of conducting the disinfection experiment, the pores of the MK−Ag foam sample were not clogged. In addition, no physical disintegration of the foams was observed. The micrographs are shown in Figure 2b,c.

3.5. Quantitative PCR and Metagenomic Sequencing.

To better understand how the prepared MK-based geopolymer foams MK and MK−Ag altered the bacterial abundance and microbiome composition, we quantified the 16S rRNA gene using qPCR and characterized the entire microbiome composition using short-read metagenomic sequencing. We determined the microbial community (bacteria and archaea) composition using metaphlan4 and annotated ARGs and MBRGs using the ResFinder and BacMet2 databases, respectively. As sequencing data are compositional by nature,[70] we combined the 16S rRNA gene copy numbers obtained from qPCR with the microbial abundances obtained from the metagenomic sequencing to determine and compare the absolute abundances of the microbial taxa in our samples. Microbial species can have several copies of the 16S rRNA gene, and the number of copies is, at best, an approximation of the total abundance. However, we do not expect the average number of copies per cell to change dramatically among the communities in the different samples. Also, although there are tools to correct the variation in the number of copies, these tools rely on known genomes and often do not perform optimally.[71]

The treated wastewater, which was obtained from the Taskila wastewater treatment plant and used as input water in this study, exhibited a varying microbial load and heterogeneous microbiome composition during the study. This can be observed in the bacterial load measured using the 16S rRNA gene quantification [Figure 2d] and in the community composition (Figure S4, Supporting Information). In the statistical analysis, this variation in the input water was taken into consideration in the assessment of changes in the microbial number of copies using linear mixed-effect models (LMM) and considering the sampling week as a random effect. Based on the LMM and posthoc tests, both types of foam samples were capable of reducing the microbial load in the input water (MK: log fold change −1.07, p-value <0.01; MK−Ag: log fold change −1.57, p-value <0.001, Table S4 in Supporting Information). Although MK−Ag achieved a better reduction in the microbial load than that achieved by MK (as measured by the 16S rRNA gene number of copies), the microbial load was not statistically significant between the effluents from these two types of foam (Table S4 in Supporting Information). The reduction in the total microbial load was less than the viable *E. coli* reduction presented in this study or the reduction in intestinal enterococci using similar types of foam reported earlier.[14] As molecular methods do not differentiate between live and dead cells and the number of bacteria mentioned above is only a minor fraction of the total community, which can include resilient members, this is somewhat expected. The foam samples prepared in this study achieved similar results in reducing the ARG and MBRG abundances [Figure 2d and Table S4 in Supporting Information]. The reduction effect of the foam without Ag was insignificant only for the ARGs (log fold change of −0.84, p-value = 0.07).

In addition to the overall reduction in the microbial load, the MK-based foam samples changed the microbial community composition of the input wastewater. The ordination plots clearly showed that the community composition of the input wastewater varied between weeks and that the change after filtration was robust over the weeks (Figure S4 in Supporting Information). We tested the changes in the community composition, antibiotic resistome, and metal and biocide resistome using a permutational multivariate analysis of variance with permutations restricted to each week due to the heterogeneity of the initial material. The results were in line with those obtained for the total abundances. In all cases, the MK-based foam sample with Ag had a significant effect on the microbiome. The change in the community composition was insignificant only in the case of the antibiotic resistome and the MK foam-based filter without Ag. The microbiome exhibited no difference in the community composition, antibiotic resistome, or metal and biocide resistome between the MK and MK−Ag foam samples (Table S5 and Figure S5 in Supporting Information).

Although the MK foam-based filters reduced the overall abundance of microbial taxa, ARGs, and MBRGs, our objective was to identify the microbial taxa and individual resistance genes that could be enriched during filtration. Ag resistance genes can be found in the same genetic elements as ARGs, and thus can be coselect for antibiotic resistance.[72,73] We also determined whether the MK foam-based samples with Ag would select for Ag resistance genes and whether they could have coselected for ARGs. Antibiotic resistance is of global concern, and, especially, fecal contaminated water, such as municipal wastewater, is rich in ARGs that can act as dissemination routes.[74,75] As expected from the total abundance results, both MK foam-based filters reduced the abundance of several microbial taxa and resistance genes.

https://doi.org/10.1021/acsestwater.3c00711
ACS EST Water 2024, 4, 687−697

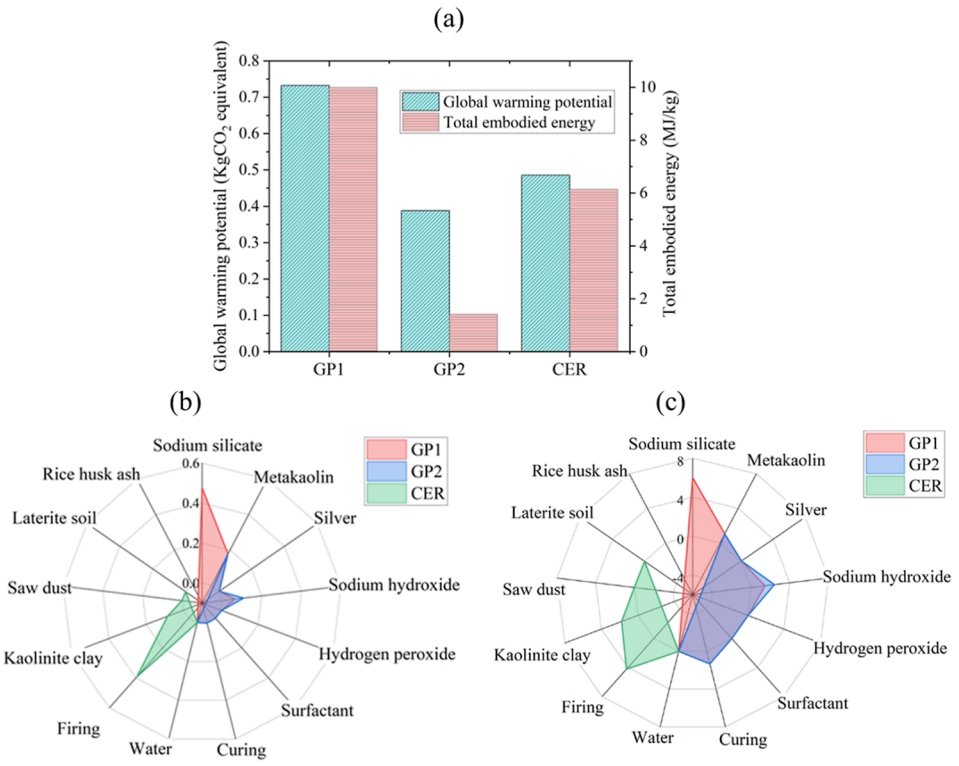

Figure 3. Global warming potential (GWP) and embodied energy (EE) for different types of water filter: (a) material and methodology contribution to the GWP in $kgCO_2$ equivalent. (b,c) EE in MJ/kg.

However, there was a clear increase in the abundance of *Ralstonia pickettii* and *Asinibacterium* sp. for both types of foam. These two taxa were not detected in the influent water but were abundant in both filtrates (Table S6 in Supporting Information). However, care should be taken when interpreting the fold changes in these taxa, as the results were based on pseudocounts added before the log transformation. These bacteria have shown tolerance to high concentrations of heavy metals and other contaminants[76,77] but their abundance was not significantly different between the filtrates, suggesting that Ag was not the selective agent for these two taxa; rather, both taxa were more abundant in foams without Ag than those with Ag, although the difference was not statistically significant. Two additional taxa were enriched, *Luteibacter anthropi* and *Aquabacterium* sp. in the filtrates obtained from the MK foam-based filters with and without Ag, respectively (Table S6 in Supporting Information).

Regarding the ARGs, only two β-lactamase genes, blaOXA-22 and blaOXA-60, were significantly enriched after the application of the MK foam without Ag. Both genes are chromosomally encoded oxacillinases from *R. pickettii*,[77,78] which explains the enrichment of these ARGs. Similarly, regarding the MBRGs, few genes were enriched due to filtration with MK foam-based filters without Ag, and most of these genes were related to heavy metal resistance systems and originated from the genus *Ralstonia* based on BacMet annotations. It is evident that the added Ag did not select for Ag resistance, and hence there was no coselection for antibiotic resistance either. The enrichment of all resistance genes detected in this study was due to the enrichment of specific taxa, rather than the selection of the genes themselves. The environmental conditions related to the selection of these specific taxa can only be speculated and further studies are needed.

3.6. Leaching of Ag, Na, Si, and Al from Foam Samples. The leaching of the main elements of the MK-based foam samples, namely, Na, Si, Al, and Ag was monitored on a daily basis until they were clearly stabilized [Figure 2e]. The leaching was measured using deionized water, which was distributed through the foam samples for approximately 5 h per day. The pH of the deionized water remained unchanged in the 8.1−8.8 range before and after distributing the deionized water through the foam samples. The leaching levels of each element stayed well below those recommended for drinking water, i.e., <100 μg/L for Ag,[79] <30−60 mg/L for Na to prevent taste,[79] and <0.2 mg/L for Al.[80] For Si, there is no recommended value. The leaching of Ag was less than that reported for a ceramic filter (a disk with a 5.1 cm diameter and a 1.5 cm thickness) coated with nano-Ag[81] and Ag nanoparticle containing a ceramic water filter.[56,82]

3.7. Life Cycle Assessment. The GWP and EE calculated for the MK−Ag, that is, an alkali-activated MK foam with an alkali activator consisting of sodium silicate and sodium hydroxide (GP1, scenario 1), a side-stream-based alkali activator, rice husk ash, and sodium hydroxide (GP2, scenario 2), and a conventional ceramic water filter (CER, scenario 3) are compared in Figure 3. The impact of a ceramic water filter on the environment is mainly caused by the calcination process (Figure 3). Compared with the ceramic filter, the alkali-activated MK foam-based water filter prepared in scenario 1 did not decrease the GWP and EE. The use of sodium silicate in scenario 1 dramatically increased the GWP and EE of the MK foam sample, which is typical with AAMs.[83] The GWP and EE in scenario 2 were smaller than those in the ceramic

https://doi.org/10.1021/acsestwater.3c00711
ACS EST Water 2024, 4, 687−697

filter. In this scenario, sodium silicate was replaced by rice husk ash and sodium hydroxide.

4. CONCLUSIONS

Alkali-activated foams, which can be used as an alternative solution to POU ceramic filters, were prepared using low-, medium-, and high-Ca aluminosilicate precursors, namely, metakaolin, a mixture of metakaolin and blast furnace slag, and blast furnace slag, respectively. The amount of H_2O_2 was optimized regarding porosity to obtain water permeability similar to that of conventional ceramic filters. The obtained compressive strength values of the optimized foam samples were 2.99, 4.58, and 5.91 MPa for MK, BFS, and BFS−MK, respectively. On the other hand, the obtained flexural strength values were 1.08, 1.54, and 2.03 MPa, respectively. Shrinkage studies showed that the BFS-based foam exhibited a higher shrinkage compared to the other two foam samples. Based on this observation, the MK-based foam was selected for modification using a colloidal Ag solution. The modified foam exhibited low leaching of Ag, Na, Si, and Al. The inactivation of *E. coli* bacteria using the MK-based foam with and without Ag was studied for 10 weeks. The inactivation performance of both foams was promising, indicating that the porosity of the foam significantly affects the inactivation along with the inactivation caused by Ag. The maximum log reduction values of the foam with and without Ag were 1.57 and 2.84, respectively. The results obtained using DNA-based methods demonstrated the efficiency of both foams (with and without Ag) in the reduction of the microbial community. LCA indicated that the MK-based foam prepared with sodium silicate does not exhibit any advantage over ceramic water filters in terms of energy consumption and carbon footprint. However, the replacement of sodium silicate with side-stream rice husk ash reduced the carbon footprint below that of a conventional ceramic water filter. The replacement of raw materials by more readily available options would also be important to enable the production of alkali-activated filters in developing countries. This study demonstrated that alkali-activated foams can be a technically and environmentally feasible alternative solution to prepared disinfecting POU ceramic filters.

■ ASSOCIATED CONTENT

Data Availability Statement

Raw data is available from an online repository: 10.23729/ce9ea927-e749-4620-9ecb-cc55c4cc94e0.

Supporting Information

The Supporting Information is available free of charge at https://pubs.acs.org/doi/10.1021/acsestwater.3c00711.

Materials and preparation; weight ratios of precursors (i.e., MK and BFS), alkali-activator solution, additional water, H_2O_2, and surfactant of different foam samples; characterization of foam samples; schematic diagram of the preparation of alkali-activated foam and Ag application; schematic diagram of the disinfection experiment; XPS spectra of Ag in MK-Ag foam before and after disinfection experiment; average physiochemical characteristics of wastewater (± standard deviation); principal coordinate analysis showing the differences in community composition, antibiotic resistome, and metal and biocide resistome between different samples, and weeks; absolute and relative abundance of 19 most abundant species; and life cycle inventory data of different materials used in geopolymer water filter and ceramic water filter (PDF)

■ AUTHOR INFORMATION

Corresponding Author

Tero Luukkonen − *Fibre and Particle Engineering Research Unit, University of Oulu, Oulu 90014, Finland;* orcid.org/0000-0002-1124-775X; Email: tero.luukkonen@oulu.fi

Authors

Mohammad Amzad Hossain Bhuyan − *Fibre and Particle Engineering Research Unit, University of Oulu, Oulu 90014, Finland;* orcid.org/0000-0003-4669-9489

Antti Karkman − *Department of Microbiology, University of Helsinki, Helsinki 00790, Finland*

Hanna Prokkola − *Research Unit of Sustainable Chemistry, University of Oulu, Oulu 90014, Finland*

Boyu Chen − *Microlab, Section of Materials and Environment, Faculty of Civil Engineering and Geosciences, Delft University of Technology, Delft 2628 CN, The Netherlands*

Priyadharshini Perumal − *Fibre and Particle Engineering Research Unit, University of Oulu, Oulu 90014, Finland*

Complete contact information is available at: https://pubs.acs.org/10.1021/acsestwater.3c00711

Author Contributions

CRediT: **Mohammad Amzad Hossain Bhuyan** conceptualization, investigation, methodology, writing-original draft; **Antti Karkman** investigation, methodology, writing-review & editing; **Hanna Prokkola** investigation, writing-review & editing; **Boyu Chen** investigation, writing-review & editing; **Priyadharshini Perumal** methodology, writing-review & editing; **Tero Luukkonen** conceptualization, methodology, project administration, supervision, writing-review & editing.

Notes

The authors declare no competing financial interest.

■ ACKNOWLEDGMENTS

This study was supported by The University of Oulu & The Academy of Finland Profi5 (grant 326291), Erkki Paasikivi Foundation (grant 20201121), and Tauno Tönning Foundation (grant 20230023). A.K. was funded by the Academy of Finland (grant 315678). The authors wish to thank Jani Österlund for his help in collecting wastewater from the Taskila wastewater treatment plant, Oulu, Finland. The authors wish to acknowledge the DNA Sequencing and Genomics Laboratory, Institute of Biotechnology, University of Helsinki, for sequencing and the CSC−IT Center for Science, Finland, for providing computational resources. Authors are grateful to Professor Mirja Illikainen for her contribution to funding acquisition.

■ REFERENCES

(1) World Health Organization. Drinking-water. https://www.who.int/news-room/fact-sheets/detail/drinking-water (accessed Feb 02, 2023).

(2) van der Laan, H.; van Halem, D.; Smeets, P. W. M. H.; Soppe, A. I. A.; Kroesbergen, J.; Wubbels, G.; Nederstigt, J.; Gensburger, I.; Heijman, S. G. J. Bacteria and Virus Removal Effectiveness of Ceramic Pot Filters with Different Silver Applications in a Long Term Experiment. *Water Res.* **2014**, *51*, 47−54.

(3) Abebe, L. S.; Su, Y.-H.; Guerrant, R. L.; Swami, N. S.; Smith, J. A. Point-of-Use Removal of Cryptosporidium Parvum from Water: Independent Effects of Disinfection by Silver Nanoparticles and Silver Ions and by Physical Filtration in Ceramic Porous Media. *Environ. Sci. Technol.* **2015**, *49* (21), 12958−12967.
(4) Farrow, C.; McBean, E.; Salsali, H. Virus Removal Efficiency of Ceramic Water Filters: Effects of Bentonite Turbidity. *Water Supply* **2014**, *14* (2), 304−311.
(5) Salsali, H.; McBean, E.; Brunsting, J. Virus Removal Efficiency of Cambodian Ceramic Pot Water Purifiers. *J. Water Health* **2011**, *9* (2), 306−311.
(6) Sullivan, R. K.; Erickson, M.; Oyanedel-Craver, V. A. Understanding the Microbiological, Organic and Inorganic Contaminant Removal Capacity of Ceramic Water Filters Doped with Different Silver Nanoparticles. *Environ. Sci.: Nano* **2017**, *4* (12), 2348−2355.
(7) Ren, D.; Colosi, L. M.; Smith, J. A. Evaluating the Sustainability of Ceramic Filters for Point-of-Use Drinking Water Treatment. *Environ. Sci. Technol.* **2013**, *47* (19), 11206−11213.
(8) Yang, H.; Xu, S.; Chitwood, D. E.; Wang, Y. Ceramic Water Filter for Point-of-Use Water Treatment in Developing Countries: Principles, Challenges and Opportunities. *Front. Environ. Sci. Eng.* **2020**, *14* (5), 79.
(9) Rayner, J.; Skinner, B.; Lantagne, D. Current Practices in Manufacturing Locally-Made Ceramic Pot Filters for Water Treatment in Developing Countries. *J. Water, Sanit. Hyg. Dev.* **2013**, *3* (2), 252−261.
(10) Yang, H.; Zhu, S.; Lin, X.; Wu, J.; Du, X.; Chen, R.; Wang, Y.; Xu, S.; Hu, L.-X.; Ying, G.-G. Lanthanum (III)-Coated Ceramic Filters in Point-of-Use Water Treatment for Bacterial Removal. *ACS ES&T Water* **2022**, *2* (4), 583−592.
(11) Yang, H.; Min, X.; Wu, J.; Lin, X.; Gao, F.-Z.; Hu, L.-X.; Zhang, L.; Wang, Y.; Xu, S.; Ying, G.-G. Removal and Inactivation of Virus by Ceramic Water Filters Coated with Lanthanum (III). *ACS ES&T Water* **2022**, *2* (10), 1811−1821.
(12) Yang, H.; Min, X.; Xu, S.; Wang, Y. Lanthanum(III)-Coated Ceramics as a Promising Material in Point-of-Use Water Treatment for Arsenite and Arsenate Removal. *ACS Sustainable Chem. Eng.* **2019**, *7* (10), 9220−9227.
(13) Yang, H.; Min, X.; Xu, S.; Bender, J.; Wang, Y. Development of Effective and Fast-Flow Ceramic Porous Media for Point-of-Use Water Treatment: Effect of Pore Size Distribution. *ACS Sustainable Chem. Eng.* **2020**, *8* (6), 2531−2539.
(14) Luukkonen, T.; Bhuyan, M.; Hokajärvi, A. M.; Pitkänen, T.; Miettinen, I. T. Water Disinfection with Geopolymer-Bentonite Composite Foam Containing Silver Nanoparticles. *Mater. Lett.* **2022**, *311*, 131636.
(15) Rubio-Avalos, E.; Rubio-Avalos, J.-C. 15—Antimicrobial Alkali-Activated Materials. In *Alkali-Activated Materials in Environmental Technology Applications*; Luukkonen, T., Ed.; Woodhead Publishing Series in Civil and Structural Engineering; Woodhead Publishing, 2022; pp 333−353.
(16) Luukkonen, T. 1—Alkali-Activated Materials in Environmental Technology: Introduction. In *Alkali-Activated Materials in Environmental Technology Applications*; Luukkonen, T., Ed.; Woodhead Publishing Series in Civil and Structural Engineering; Woodhead Publishing, 2022; pp 1−12.
(17) Bai, C.; Franchin, G.; Elsayed, H.; Zaggia, A.; Conte, L.; Li, H.; Colombo, P. High-Porosity Geopolymer Foams with Tailored Porosity for Thermal Insulation and Wastewater Treatment. *J. Mater. Res.* **2017**, *32* (17), 3251−3259.
(18) Bai, C.; Colombo, P. Processing, Properties and Applications of Highly Porous Geopolymers: A Review. *Ceram. Int.* **2018**, *44* (14), 16103−16118.
(19) Franchin, G.; Pesonen, J.; Luukkonen, T.; Bai, C.; Scanferla, P.; Botti, R.; Carturan, S.; Innocentini, M.; Colombo, P. Removal of Ammonium from Wastewater with Geopolymer Sorbents Fabricated via Additive Manufacturing. *Mater. Des.* **2020**, *195*, 109006.
(20) Li, X.; Bai, C.; Qiao, Y.; Wang, X.; Yang, K.; Colombo, P. Preparation, Properties and Applications of Fly Ash-Based Porous Geopolymers: A Review. *J. Clean. Prod.* **2022**, *359*, 132043.
(21) Bhuyan, M. A. H.; Gebre, R. K.; Finnilä, M.; Illikainen, M.; Luukkonen, T. Preparation of Filter by Alkali Activation of Blast Furnace Slag and Its Application for Dye Removal. *J. Environ. Chem. Eng.* **2022**, *10* (1), 107051.
(22) Li, X.; Liu, L.; Bai, C.; Yang, K.; Zheng, T.; Lu, S.; Li, H.; Qiao, Y.; Colombo, P. Porous Alkali-Activated Material from Hypergolic Coal Gangue by Microwave Foaming for Methylene Blue Removal. *J. Am. Ceram. Soc.* **2023**, *106* (2), 1473−1489.
(23) Matalkah, F.; Khraisat, H.; Al-Momani, I. The Efficiency of Volcanic Tuff-Based Foamed Geopolymer for Heavy Metals Removal: A Parametric Study. *Int. J. Environ. Res.* **2022**, *16* (5), 67.
(24) Ramos, F. J. H. T. V.; Marques, M. d. F. V.; Rodrigues, J. G. P.; Aguiar, V. d. O.; da Luz, F. S.; de Azevedo, A. R. G.; Monteiro, S. N. Development of Novel Geopolymeric Foam Composites Coated with Polylactic Acid to Remove Heavy Metals from Contaminated Water. *Case Stud. Constr. Mater.* **2022**, *16*, No. e00795.
(25) Bhuyan, M. A. H.; Luukkonen, T. Adsorption of Methylene Blue by Composite Foams Containing Alkali-Activated Blast Furnace Slag and Lignin. *Int. J. Environ. Sci. Technol.* **2023**.
(26) O'Connor, S. J.; MacKenzie, K. J. D.; Smith, M. E.; Hanna, J. V. Ion Exchange in the Charge-Balancing Sites of Aluminosilicate Inorganic Polymers. *J. Mater. Chem.* **2010**, *20* (45), 10234−10240.
(27) Bhuyan, M. A. H.; Kurtulus, C.; Heponiemi, A.; Luukkonen, T. Peracetic Acid as a Novel Blowing Agent in the Direct Foaming of Alkali-Activated Materials. *Appl. Clay Sci.* **2023**, *231*, 106727.
(28) Kallman, E. N.; Oyanedel-Craver, V. A.; Smith, J. A. Ceramic Filters Impregnated with Silver Nanoparticles for Point-of-Use Water Treatment in Rural Guatemala. *J. Environ. Eng.* **2011**, *137* (6), 407−415.
(29) Oyanedel-Craver, V. A.; Smith, J. A. Sustainable Colloidal-Silver-Impregnated Ceramic Filter for Point-of-Use Water Treatment. *Environ. Sci. Technol.* **2008**, *42* (3), 927−933.
(30) International Organization for Standardization. Water Quality—Application of Inductively Coupled Plasma Mass Spectrometry (ICP-MS)—Part 2: Determination of 62 Elements. 2016, https://www.iso.org/standard/62962.html (accessed April 27, 2023).
(31) International Organization for Standardization. Water Quality—Enumeration of Escherichia Coli and Coliform Bacteria—Part 1: Membrane Filtration Method for Waters with Low Bacterial Background Flora. 2014, https://www.iso.org/standard/55832.html (accessed Jan 14, 2023).
(32) Edwards, U.; Rogall, T.; Blocker, H.; Emde, M.; Bottger, E. C. Isolation and Direct Complete Nucleotide Determination of Entire Genes - Characterization of a Gene Coding for 16S-Ribosomal RNA. *Nucleic Acids Res.* **1989**, *17* (19), 7843−7853.
(33) Muyzer, G.; de Waal, E. C.; Uitterlinden, A. G. Profiling of Complex Microbial Populations by Denaturing Gradient Gel Electrophoresis Analysis of Polymerase Chain Reaction-Amplified Genes Coding for 16S rRNA. *Appl. Environ. Microbiol.* **1993**, *59* (3), 695−700.
(34) Ruuskanen, M.; Muurinen, J.; Meierjohan, A.; Pärnänen, K.; Tamminen, M.; Lyra, C.; Kronberg, L.; Virta, M. Fertilizing with Animal Manure Disseminates Antibiotic Resistance Genes to the Farm Environment. *J. Environ. Qual.* **2016**, *45* (2), 488−493.
(35) Martin, M. Cutadapt Removes Adapter Sequences from High-Throughput Sequencing Reads. *EMBnet J.* **2011**, *17* (1), 10.
(36) Blanco-Miguez, A.; Beghini, F.; Cumbo, F.; McIver, L. J.; Thompson, K. N.; Zolfo, M.; Manghi, P.; Dubois, L.; Huang, K. D.; Thomas, A. M.; Piccinno, G.; Piperni, E.; Punčochář, M.; Valles-Colomer, M.; Tett, A.; Giordano, F.; Davies, R.; Wolf, J.; Berry, S. E.; Spector, T. D.; Franzosa, E. A.; Pasolli, E.; Asnicar, F.; Huttenhower, C.; Segata, N. Extending and Improving Metagenomic Taxonomic Profiling with Uncharacterized Species with MetaPhlAn 4. *bioRxiv* **2022**, 2022.08.22.504593. preprint
(37) Zankari, E.; Hasman, H.; Cosentino, S.; Vestergaard, M.; Rasmussen, S.; Lund, O.; Aarestrup, F. M.; Larsen, M. V.

Identification of Acquired Antimicrobial Resistance Genes. *J. Antimicrob. Chemother.* **2012**, *67* (11), 2640−2644.
(38) Langmead, B.; Salzberg, S. L. Fast Gapped-Read Alignment with Bowtie 2. *Nat. Methods* **2012**, *9* (4), 357−359.
(39) Li, H.; Handsaker, B.; Wysoker, A.; Fennell, T.; Ruan, J.; Homer, N.; Marth, G.; Abecasis, G.; Durbin, R. The Sequence Alignment/Map format and SAMtools. *Bioinformatics* **2009**, *25* (16), 2078−2079.
(40) Buchfink, B.; Xie, C.; Huson, D. H. Fast and Sensitive Protein Alignment Using DIAMOND. *Nat. Methods* **2015**, *12* (1), 59−60.
(41) Pal, C.; Bengtsson-Palme, J.; Rensing, C.; Kristiansson, E.; Larsson, D. G. J. BacMet: Antibacterial Biocide and Metal Resistance Genes Database. *Nucleic Acids Res.* **2014**, *42*, D737−D743.
(42) R Core Team. *R: A Language and Environment for Statistical Computing*; R Foundation for Statistical Computing: Vienna, Austria, 2016.
(43) Bates, D.; Mächler, M.; Bolker, B.; Walker, S. Fitting Linear Mixed-Effects Models Using **Lme4**. *J. Stat. Software* **2015**, *67* (1), 1−48.
(44) Hothorn, T.; Bretz, F.; Westfall, P. Simultaneous Inference in General Parametric Models. *Biom. J.* **2008**, *50* (3), 346−363.
(45) Oksanen, J.; Simpson, G. L.; Blanchet, F. G.; Kindt, R.; Legendre, P.; Minchin, P. R.; O'Hara, R. B.; Solymos, P.; Stevens, M. H. H.; Szoecs, E.; Wagner, H.; Barbour, M.; Bedward, M.; Bolker, B.; Borcard, D.; Carvalho, G.; Chirico, M.; Caceres, M. D.; Durand, S.; Evangelista, H. B. A.; FitzJohn, R.; Friendly, M.; Furneaux, B.; Hannigan, G.; Hill, M. O.; Lahti, L.; McGlinn, D.; Ouellette, M.-H.; Cunha, E. R.; Smith, T.; Stier, A.; Braak, C. J. F. T.; Weedon, J. *Vegan: Community Ecology Package*, 2022.
(46) Mallick, H.; Rahnavard, A.; McIver, L. J.; Ma, S.; Zhang, Y.; Nguyen, L. H.; Tickle, T. L.; Weingart, G.; Ren, B.; Schwager, E. H.; Chatterjee, S.; Thompson, K. N.; Wilkinson, J. E.; Subramanian, A.; Lu, Y.; Waldron, L.; Paulson, J. N.; Franzosa, E. A.; Bravo, H. C.; Huttenhower, C. Multivariable Association Discovery in Population-Scale Meta-Omics Studies. *PLoS Comput. Biol.* **2021**, *17* (11), No. e1009442.
(47) Wickham, H. *Ggplot2: Elegant Graphics for Data Analysis*; Springer-Verlag New York, 2009.
(48) Pedersen, T. L. *Patchwork: The Composer of Plots*, 2022.
(49) Barnett, D.; Arts, I.; Penders, J. microViz: An R Package for Microbiome Data Visualization and Statistics. *J. Open Source Softw.* **2021**, *6* (63), 3201.
(50) ISO. ISO 14040:2006 Environmental Management—Life Cycle Assessment—Principles and Framework—AMENDMENT 1. 2006, https://www.iso.org/standard/37456.html (accessed May 16, 2023).
(51) EN. EN 15804:2012+A2:2019 Sustainability of Construction Works. Environmental Product Declarations. Core Rules for the Product Category of Construction Products. 2012, https://www.en-standard.eu/bs-en-15804-2012-a2-2019-sustainability-of-construction-works-environmental-product-declarations-core-rules-for-the-product-category-of-construction-products/ (accessed May 16, 2023).
(52) Hanwright, J.; Zhou, J.; Evans, G. M.; Galvin, K. P. Influence of Surfactant on Gas Bubble Stability. *Langmuir* **2005**, *21* (11), 4912−4920.
(53) Qiao, Y.; Li, X.; Bai, C.; Li, H.; Yan, J.; Wang, Y.; Wang, X.; Zhang, X.; Zheng, T.; Colombo, P. Effects of Surfactants/Stabilizing Agents on the Microstructure and Properties of Porous Geopolymers by Direct Foaming. *J. Asian Ceram. Soc.* **2021**, *9* (1), 412−423.
(54) Luukkonen, T.; Yliniemi, J.; Sreenivasan, H.; Ohenoja, K.; Finnilä, M.; Franchin, G.; Colombo, P. Ag- or Cu-Modified Geopolymer Filters for Water Treatment Manufactured by 3D Printing, Direct Foaming, or Granulation. *Sci. Rep.* **2020**, *10* (1), 7233.
(55) Rayner, J.; Zhang, H.; Schubert, J.; Lennon, P.; Lantagne, D.; Oyanedel-Craver, V. Laboratory Investigation into the Effect of Silver Application on the Bacterial Removal Efficacy of Filter Material for Use on Locally Produced Ceramic Water Filters for Household Drinking Water Treatment. *ACS Sustainable Chem. Eng.* **2013**, *1* (7), 737−745.
(56) Shepard, Z. J.; Lux, E. M.; Oyanedel-Craver, V. A. Performance of Silver Nanoparticle-Impregnated Ovoid Ceramic Water Filters. *Environ. Sci.: Nano* **2020**, *7* (6), 1772−1780.
(57) van Halem, D.; van der Laan, H.; Heijman, S. G. J.; van Dijk, J. C.; Amy, G. L. Assessing the Sustainability of the Silver-Impregnated Ceramic Pot Filter for Low-Cost Household Drinking Water Treatment. *Phys. Chem. Earth, Parts A/B/C* **2009**, *34* (1−2), 36−42.
(58) Luukkonen, T.; Olsen, E.; Turkki, A.; Muurinen, E. Ceramic-like Membranes without Sintering via Alkali Activation of Metakaolin, Blast Furnace Slag, or Their Mixture: Characterization and Cation-Exchange Properties. *Ceram. Int.* **2023**, *49* (7), 10645−10651.
(59) Ridtirud, C.; Chindaprasirt, P.; Pimraksa, K. Factors Affecting the Shrinkage of Fly Ash Geopolymers. *Int. J. Miner. Metall. Mater.* **2011**, *18* (1), 100−104.
(60) Segura, I. P.; Luukkonen, T.; Yliniemi, J.; Sreenivasan, H.; Damø, A. J.; Jensen, L. S.; Canut, M.; Kantola, A. M.; Telkki, V.-V.; Jensen, P. A. Comparison of One-Part and Two-Part Alkali-Activated Metakaolin and Blast Furnace Slag. *J. Sustain. Metall.* **2022**, *8* (4), 1816−1830.
(61) Masturi; Silvia; Aji, M. P.; Sustini, E.; Khairurrijal; Abdullah, M. Permeability, Strength and Filtration Performance for Uncoated and Titania-Coated Clay Wastewater Filters. *Am. J. Environ. Sci.* **2012**, *8* (2), 79−94.
(62) Omoniyi, O. A.; Salifu, A. A.; Obayemi, J. D.; Oyewole, O. K.; Nigay, P.-M.; Akin-Ojo, O.; Soboyejo, W. O. Effects of Sintering Temperature on the Filtration and Mechanical Properties of Ceramic Water Filters. *Cogent Eng.* **2022**, *9* (1), 2119536.
(63) Oyanedel-Craver, V.; Narkiewicz, S.; Genovesi, R.; Bradshaw, A.; Cardace, D. Effect of Local Materials on the Silver Sorption and Strength of Ceramic Water Filters. *J. Environ. Chem. Eng.* **2014**, *2* (2), 841−848.
(64) Salvini, V. R.; Luchini, B.; Aneziris, C. G.; Pandolfelli, V. C. Innovation in Ceramic Foam Filters Manufacturing Process. *Int. J. Appl. Ceram. Technol.* **2019**, *16* (1), 378−388.
(65) Shivaraju, H. P.; Egumbo, H.; Madhusudan, P.; Anil Kumar, K. M.; Midhun, G. Preparation of Affordable and Multifunctional Clay-Based Ceramic Filter Matrix for Treatment of Drinking Water. *Environ. Technol.* **2019**, *40* (13), 1633−1643.
(66) Jaya, N. A.; Yun-Ming, L.; Cheng-Yong, H.; Abdullah, M. M. A. B.; Hussin, K. Correlation between Pore Structure, Compressive Strength and Thermal Conductivity of Porous Metakaolin Geopolymer. *Constr. Build. Mater.* **2020**, *247*, 118641.
(67) Huang, D.; Chen, P.; Peng, H.; Yuan, Q.; Tian, X. Drying Shrinkage Performance of Medium-Ca Alkali-Activated Fly Ash and Slag Pastes. *Cem. Concr. Compos.* **2022**, *130*, 104536.
(68) Dagher, L. A.; Hassan, J.; Kharroubi, S.; Jaafar, H.; Kassem, I. I. Nationwide Assessment of Water Quality in Rivers across Lebanon by Quantifying Fecal Indicators Densities and Profiling Antibiotic Resistance of Escherichia Coli. *Antibiotics* **2021**, *10* (7), 883.
(69) Bielefeldt, A. R.; Kowalski, K.; Summers, R. S. Bacterial Treatment Effectiveness of Point-of-Use Ceramic Water Filters. *Water Res.* **2009**, *43* (14), 3559−3565.
(70) Quinn, T. P.; Erb, I.; Richardson, M. F.; Crowley, T. M. Understanding Sequencing Data as Compositions: An Outlook and Review. *Bioinformatics* **2018**, *34* (16), 2870−2878.
(71) Louca, S.; Doebeli, M.; Parfrey, L. W. Correcting for 16S rRNA Gene Copy Numbers in Microbiome Surveys Remains an Unsolved Problem. *Microbiome* **2018**, *6* (1), 41.
(72) Seiler, C.; Berendonk, T. U. Heavy Metal Driven Co-Selection of Antibiotic Resistance in Soil and Water Bodies Impacted by Agriculture and Aquaculture. *Front. Microbiol.* **2012**, *3*, 399.
(73) Vats, P.; Kaur, U. J.; Rishi, P. Heavy Metal-Induced Selection and Proliferation of Antibiotic Resistance: A Review. *J. Appl. Microbiol.* **2022**, *132* (6), 4058−4076.
(74) Baquero, F.; Martinez, J.; Canton, R. Antibiotics and Antibiotic Resistance in Water Environments. *Curr. Opin. Biotechnol.* **2008**, *19* (3), 260−265.

https://doi.org/10.1021/acsestwater.3c00711
ACS EST Water 2024, 4, 687−697

(75) Karkman, A.; Pärnänen, K.; Larsson, D. G. J. Fecal Pollution Can Explain Antibiotic Resistance Gene Abundances in Anthropogenically Impacted Environments. *Nat. Commun.* **2019**, *10* (1), 80.
(76) Brzoska, R. M.; Huntemann, M.; Clum, A.; Chen, A.; Kyrpides, N.; Palaniappan, K.; Ivanova, N.; Mikhailova, N.; Ovchinnikova, G.; Varghese, N.; Mukherjee, S.; Reddy, T. B. K.; Daum, C.; Shapiro, N.; Woyke, T.; Bollmann, A. Complete Genome Sequence for *Asinibacterium* Sp. Strain OR53 and Draft Genome Sequence for *Asinibacterium* Sp. Strain OR43, Two Bacteria Tolerant to Uranium. *Microbiol. Resour. Announce.* **2019**, *8* (14), No. e01701−18.
(77) Kim, S. G.; Summage-West, C. V.; Buzatu, D. A.; Foley, S. L. Draft Genome Sequence of Ralstonia Pickettii Strain NCTR106, Isolated from Milk Carton Paperboard. *Microbiol. Resour. Announce.* **2022**, *11* (2), No. e01084−21.
(78) Girlich, D.; Naas, T.; Nordmann, P. OXA-60, a Chromosomal, Inducible, and Imipenem-Hydrolyzing Class D β-Lactamase from *Ralstonia Pickettii*. *Antimicrob. Agents Chemother.* **2004**, *48* (11), 4217−4225.
(79) US EPA. *2018 Drinking Water Standards and Advisory Tables*; US EPA. https://19january2021snapshot.epa.gov/sdwa/2018-drinking-water-standards-and-advisory-tables (accessed Dec 09, 2022).
(80) World Health Organization. *Guidelines for Drinking-Water Quality*; World Health Organization, 2011. https://apps.who.int/iris/handle/10665/44584 (accessed Dec 09, 2022).
(81) Mittelman, A. M.; Lantagne, D. S.; Rayner, J.; Pennell, K. D. Silver Dissolution and Release from Ceramic Water Filters. *Environ. Sci. Technol.* **2015**, *49* (14), 8515−8522.
(82) Ngoc Dung, T. T.; Phan Thi, L.-A.; Nam, V. N.; Nhan, T. T.; Quang, D. V. Preparation of Silver Nanoparticle-Containing Ceramic Filter by in-Situ Reduction and Application for Water Disinfection. *J. Environ. Chem. Eng.* **2019**, *7* (3), 103176.
(83) Abdulkareem, M.; Havukainen, J.; Horttanainen, M. 17—Environmental Performance of Alkali-Activated Materials in Environmental Technology Applications. In *Alkali-Activated Materials in Environmental Technology Applications*; Luukkonen, T., Ed.; Woodhead Publishing Series in Civil and Structural Engineering; Woodhead Publishing, 2022; pp 383−405.

https://doi.org/10.1021/acsestwater.3c00711
ACS EST Water 2024, 4, 687−697